

# Thermal and Magnetic Properties of the Spin-Chain Material, $\text{Pr}_3\text{RuO}_7$

M. Freamat, X.N. Lin, V. Durairaj, S. Chikara, G. Cao, and J.W. Brill

Department of Physics and Astronomy, University of Kentucky, Lexington, KY 40506-0055

## ABSTRACT

We present measurements of the magnetic moment and specific heat of single crystals of the spin-chain insulator,  $\text{Pr}_3\text{RuO}_7$ . The susceptibility indicates that three-dimensional antiferromagnetic order sets in at  $T_N = 54$  K, with spin polarization approximately along the chain direction, but the susceptibility anisotropy above  $T_N$  indicates that the intrachain interactions are predominantly ferromagnetic while the interchain interactions are antiferromagnetic. This competition presumably gives rise to the observed metamagnetic behavior for applied fields along the polarization direction. The specific heat anomaly at  $T_N$  is unusually mean-field in shape, with magnitude indicating that the transition involves mostly ordering of the ruthenium moments. A Schottky-like anomaly at low temperature may be due to praesodymium ions ordering in the effective field established at  $T_N$ .

PACS numbers: 75.40.Cx, 75.50.Ee

## 1. Introduction

Ruthenium-based oxides provide an excellent opportunity to study novel electronic and magnetic states. In this paper, we report our experimental investigation of the magnetic and calorimetric properties of high-quality single-crystals of  $\text{Pr}_3\text{RuO}_7$ . This compound belongs to a class of ruthenates with formula  $\text{Ln}_3\text{RuO}_7$  (Ln for lanthanides) with fluorite-related phases, either crystallizing in the *Cmcm* space group of the orthorhombic system or in a disordered fluorite-phase, depending on the size of the Ln cations relative to pentavalent cation  $\text{Ru}^{1-4}$ .

It was shown<sup>5-7</sup> that the Pr cation is large enough for  $\text{Pr}_3\text{RuO}_7$  to crystallize in the ordered phase. Its crystalline structure is layered along *a*-axis, each *bc*-plane layer containing chains of corner-sharing  $\text{RuO}_6$  octahedra zigzagging along *c*-axis, flanked by edge-sharing eightfold coordinated  $\text{PrO}_8$  distorted cubes involving one third of the Pr ions. The other two thirds of the Pr ions, with sevenfold oxygen coordination, are between the layers. The layer separation is about 5.5 Å, significantly larger than the intra-layer chain separation of about 3.7 Å. This characterizes an almost one-dimensional configuration and it is one of the reasons these materials attracted attention, since their anisotropy could translate into specific magnetic and electronic properties due to the dependency of electron magnetic coupling on the crystal directions. For example, spin density waves<sup>8</sup>, spin-Peierls transitions<sup>9</sup> or the Haldane-gap opening in an integer-spin Heisenberg antiferromagnet<sup>10</sup> are phenomena associated with low dimensional spin systems. Another reason for studying the  $\text{Pr}_3\text{RuO}_7$  ruthenate is the presence of multiple magnetic constituents: the common highly oxidized  $\text{Ru}^{5+}$  4d cations (spin S=3/2) could experience spin interactions with the magnetically active  $\text{Pr}^{3+}$  ions, in addition to the intra-chain coupling and the degeneracy removing interaction with the crystalline electric field.

Previous measurements on this material were on powdered samples. The present measurements were on single crystal samples for which, in principle, the lower density of sinks for vacancies (such as grain boundaries or dislocations) and resulting less clustered distribution should decrease the impurity contribution and hence favor the intrinsic features compared to polycrystalline samples.

Single crystals of  $\text{Pr}_3\text{RuO}_7$  were synthesized by the floating zone technique using a commercial image furnace (NEC-SC II). The starting materials were  $\text{Pr}_6\text{O}_{11}$  and  $\text{RuO}_2$  powders with atomic ratio of 2.7:1. The mixture of  $\text{RuO}_2$  and  $\text{Pr}_6\text{O}_{11}$  was ground in a mortar and preheated at 900°C in air for 15hrs. The heated powder was then reground and formed into a rod 6mm in diameter and 70mm in length using hydrostatic pressure, which was sintered in air at 900°C for 15hrs. After these initial heat treatments, crystals were grown in the image furnace, under  $\text{O}_2$  pressure of around 0.25 MPa. The single crystals obtained from this growth were characterized by powder X-ray diffraction and energy dispersive X-ray spectroscopy. All results indicate that the crystals are single phase with lattice parameters ( $a=10.9802 \text{ \AA}$ ,  $b=7.3839 \text{ \AA}$ ,  $c=7.5304 \text{ \AA}$ ) consistent with published values<sup>5,6</sup>.

## 2. Magnetic Properties

The magnetic properties of the  $\text{Pr}_3\text{RuO}_7$  single crystals were measured using a Quantum Design MPMS LX 7T SQUID magnetometer, with the field aligned approximately parallel or perpendicular to the crystalline c-axis. The direction of the field in the ab-plane was not determined. The results shown below were for an irregularly shaped crystal of mass 0.8 mg; similar results were obtained for other samples.

Shown in Fig.1a is the magnetic susceptibility  $\chi$  (defined as  $M/B$  in the low field limit) as a function of temperature for fields  $B=0.01$  T parallel and perpendicular to the  $c$ -axis. The susceptibility is strongly anisotropic, with  $\chi_{\parallel} > \chi_{\perp}$  at high temperatures, indicating that the easy axis for the spin polarization is along the  $\text{RuO}_6$  and  $\text{PrO}_8$  chains. Also as expected, the two components of the susceptibility bracket that measured for powder samples<sup>6,7</sup>. There is a sharp peak in  $\chi_{\parallel}$  and cusp in  $\chi_{\perp}$  at 54 K that defines the Neel temperature,  $T_N$ , i.e. the onset of antiferromagnetic order, with the magnetization of the sublattices again (approximately) along the chain direction. Note that while antiferromagnetic ordering at  $T_N=54$  K is consistent with that seen in polycrystalline samples<sup>5-7</sup>, the data in Fig.1a shows no sign of a second, weaker magnetic ordering ( $\sim 35$  K) observed in the polycrystalline samples<sup>6,7</sup>. While the origin of the discrepancy is not entirely clear, it cannot be ruled out that this anomaly is not intrinsic to the material but due to crystalline defects affecting the spin structure.

As mentioned above, the crystal structure features a zigzag chain of corner-sharing  $\text{RuO}_6$  octahedra and a row of edged-sharing  $\text{PrO}_8$  pseudocubes that alternately run along the  $c$ -axis<sup>5,6</sup>. Hence, the magnetic interaction along the  $c$ -axis is expected to be stronger than for other directions. The magnetic interactions of the interlayer praesodymium ions are expected to be weak, since the ionic spacing is large and there are not oxygen ions appropriate as intermediaries for superexchange<sup>6</sup>. Furthermore, the interaction may be governed primarily by the Ru d-electrons, since the corner-shared octahedra, with  $\sim 180^{\circ}$ -Ru-O-Ru bond angles, are much more favorable for superexchange interactions than the edge-shared pseudocubes, with  $\sim 90^{\circ}$ -Pr-O-Pr bond angles. For example, it was found that doping on the ruthenium sites much more strongly affects the phase transition than doping on the praesodymium sites<sup>7</sup>; in addition, the specific heat

anomaly, discussed below, also suggests that the transition involves ordering of the ruthenium spins. Of course, interchain magnetic coupling, e.g. between Ru and Pr chains<sup>6</sup> along the b-axis, is needed to drive the phase transition.

The complexity of the spin structure, and unconventional nature of the antiferromagnetism are expected to be born out by measurements of the susceptibility anisotropy in the ab-plane. In particular, in preliminary measurements we have observed that rather than a cusp, a small peak is observed at  $T_N$  for most in-plane directions; i.e. there seems to be a unique “hard-axis” rather than “hard-plane”, as for conventional antiferromagnets. This issue is being further investigated.

The unconventional magnetic interactions are also indicated by the high temperature susceptibility. For temperatures between 150 K and 350 K, the susceptibility is an excellent fit to the Curie-Weiss law [ $\chi = \chi_0 + C/(T - \theta_C)$ ], as shown in the inset to Figure 1a, where  $(\chi - \chi_0)^{-1}$  vs. T is plotted. The fitting parameters are the temperature independent term,  $\chi_0 = 1.74 \text{ memu}\cdot\text{mol}^{-1}$  for the c-axis and  $2.29 \text{ memu}\cdot\text{mol}^{-1}$  for the perpendicular direction, the Curie temperature  $\theta_C = +48 \text{ K}$  for the c-axis and  $-21 \text{ K}$  for the perpendicular direction, and the Curie constant  $C = 4.21 \text{ emu K mol}^{-1}$  for both directions, corresponding to an effective moment,  $\mu_{\text{eff}} = 5.81 \mu_B$ , where  $\mu_B$  is the Bohr magneton. It is remarkable that  $\theta_C$  is negative for the perpendicular direction and positive (and larger) for the c-axis, as shown in the inset of Fig.1a, (Note that polycrystalline samples have a small, positive  $\theta_C$ .<sup>5-7</sup>) This indicates that the exchange coupling is antiferromagnetic for the perpendicular direction and ferromagnetic and twice as strong for the c-axis. Such anisotropic behavior again suggests that the intra-chain coupling in the RuO<sub>6</sub> octahedra is primarily responsible for the magnetic interactions along the c-axis, whereas the

alternating  $\text{RuO}_6$  and  $\text{PrO}_8$  chains facilitate weaker, yet significant inter-chain interactions or d-f electron coupling in the ab-plane.

The Curie constant is somewhat smaller than those obtained from the polycrystalline samples ( $5.4\text{-}6.0 \text{ emu}\cdot\text{K}\cdot\text{mol}^{-1}$ )<sup>5-7</sup>, which may in part be due to the analysis, e.g. temperature ranges of the fits. More importantly, the constants for free  $\text{Pr}^{3+}$  ( $J=4$ ) and  $\text{Ru}^{5+}$  ( $S=3/2$ ) ions are expected to be  $1.56 \mu_B$  and  $1.87 \text{ emu}\cdot\text{K}\cdot\text{mol}^{-1}$ , respectively, so the Curie constant expected for  $\text{Pr}_3\text{RuO}_7$  is  $6.6 \text{ emu}\cdot\text{K}\cdot\text{mol}^{-1}$  if the free moments are unquenched. The smaller observed Curie constant implies that the crystalline electric field is quenching the orbital angular momentum, and reducing the moment, of at least some of Pr ions<sup>7</sup>; e.g if the Pr ions have  $\mu_{\text{eff}} = 2.8 \mu_B$  (i.e  $S=1, L=0$ ), the expected Curie constant will be  $4.9 \text{ emu}\cdot\text{K}\cdot\text{mol}^{-1}$ , close to the observed value.

The significance of the temperature independent term ( $\chi_0$ ) is not understood; it was not observed in References [5, 6]. Its value is similar to that of conducting ruthenates, suggesting that while there is a sizable density of states in  $\text{Pr}_3\text{RuO}_7$ , its insulating character reflects localization due to strong scattering rather than a band or correlation gap. However, it is more likely that  $\chi_0$  reflects the van Vleck contribution of the praesodymium ions with partially quenched orbital moments. In addition, the upturn in  $\chi$  seen at low temperatures does not follow a Curie-Weiss law and its origin is also unclear.

The magnetic anisotropy is well illustrated in isothermal magnetization,  $M$ . Shown in Fig. 2 is  $M(B)$  at  $T=2 \text{ K}$  for the c-axis and the perpendicular direction (i.e. that of Figure 1 for which the cusp in  $\chi$  is observed). The most remarkable feature is that while  $M_{\perp}$  remains paramagnetic, there is an abrupt rise in  $M_{\parallel}$ , which marks a metamagnetic transition at  $B_c=3.5 \text{ T}$ , a reversal of the local spin directions that changes the magnetic state from antiferromagnetic to ferromagnetic via a first order transition. (For other directions in the ab-plane, behavior

intermediate between  $M_{\parallel}$  and  $M_{\perp}$  are observed.) A metamagnetic transition occurs in an antiferromagnet that has both strong anisotropy and competing ferromagnetic interactions<sup>11</sup>, as we observe. It is interesting, therefore, that  $\text{La}_3\text{RuO}_7$ , with only a single magnetic species, exhibits a spin-flop (i.e. rotation of the spin-sublattice polarization) rather than a metamagnetic transition in a magnetic field<sup>4</sup>. As shown in Figure 2, the saturation moment of our  $\text{Pr}_3\text{RuO}_7$  crystal is  $M_s = 4.8 \mu_B/\text{f.u.}$  at  $T = 2\text{K}$ ; with increasing temperature,  $M_s$  decreases slowly and the transition broadens<sup>7</sup>. Assuming a zero orbital contribution to the ruthenium moment,  $M_s$  ( $=4.80 \mu_B/\text{f.u.}$ ) is larger than that expected for the  $\text{Ru}^{5+}$  ion ( $3 \mu_B$ ) alone, but much smaller than the combined moment of the Ru and Pr ions ( $12.6 \mu_B$  assuming a free ( $J=4$ ) praeodynium moment of  $3.2 \mu_B$  and  $8\mu_B$  assuming  $S=1$  and full orbital moment quenching of the praeodyniums). That  $M_s$  is intermediate between  $M_s$  (Ru) and  $M_s$  (Ru+Pr) may signal a subtle d-f coupling, which may be facilitated by the metamagnetic transition, i.e., the internal magnetic field created by the fully polarized spins of the ruthenium 4d chains but not that of the interlayer ions. It is also noted that there appears to be an additional anomaly in  $M$  at  $B=3.9 \text{ T}$ , which is absent in polycrystalline samples, i.e. the spin polarization occurs in steps.

### 3. Specific Heat

For heat-capacity measurements, we used the ac-calorimetry technique with chopped light as the heating source<sup>12</sup>. Since the incident power is unknown, only relative values of the heat capacity were obtained, so the specific heat ( $c_p$ ) was normalized using higher-temperature values obtained with differential scanning calorimetry<sup>13</sup>. In the 15-250 K temperature range, the measurements were performed on a 21 mg sample mounted on a thermocouple thermometer,

while in the 3-20 K range the sample was mounted on a cernox bolometer. (Note that in both cases the heat capacity of the thermometer was much less than that of the sample.) The chopping frequency  $\omega$  was tested and adjusted in different temperature intervals to be between the internal and external relaxation times. Typically,  $\omega/2\pi \approx 4$  Hz for thermocouple based measurements and  $\omega/2\pi \approx 10$  Hz in the temperature range using the bolometer. We did not observe any significant frequency dependence or hysteretic dependence on temperature. The inset to Figure 3 shows the specific heat, normalized to the gas constant  $R = 8.31 \text{ J}\cdot\text{mol}^{-1}\cdot\text{K}^{-1}$ , as a function of temperature, with the normalizing DSC data. Note that at room temperature the specific heat is  $\sim 90\%$  of its Dulong-Petit value ( $33R$ ), as expected.

We also attempted measurements on the 0.8 mg sample of Figures 1-2, but the internal and external time constants were too close for quantitative measurements. The results, however, were qualitatively similar to those of the larger sample.

Figure 3 shows the specific heat between 20 K and 80 K; a large anomaly is observed at  $T_N \approx 53$  K. As for the susceptibility, we do not observe a second anomaly at  $T = 35$  K; whereas a  $\Delta c_P \sim 0.7R$  anomaly was observed at 35 K by Harada and Hinatsu<sup>6</sup>, our noise level gives  $\Delta c_P < 0.03R$  at this temperature. Otherwise, our anomaly  $T_N$  is very similar in shape and size to that of Reference [6]. In particular, the anomaly is surprisingly “mean-field” in shape, not only in being much steeper (i.e. “vertical”) on its high temperature side than on its low-temperature side, but in only extrapolating to its background value (estimated by the smooth curve discussed below) at  $T \sim T_N / 2$ . Of course, mean-field specific heat anomalies are unusual for Neel transitions in localized systems, suggesting that the magnetic interactions in  $\text{Pr}_3\text{RuO}_7$  are unusually long-range. Hence our observed anomaly,  $\Delta c_P \sim 2R$ , should be considered an upper limit to its mean-field value.

In mean-field theory, the anomaly for  $v_N$  ordering spins/formula unit is given by<sup>14</sup>

$\Delta c_{MF} = (5 v_N R/2) (g_J^2 - 1) / (g_J^2 + 1)$ , where  $g_J$  is the relevant spin degeneracy. In related  $Ln_3RuO_7$  lanthanide compounds, Harada *et al*<sup>2,4</sup> argue that the crystal field reduces the ground state degeneracy of both the rare earth and ruthenium ions to  $g_J = 2$ . Hence, if only the ruthenium spins order in zero field at  $T_N$ ,  $\Delta c_{MF}$  would be between 1.5 R ( $g_J = 2$ ) and 2.2 R ( $g_J = 4$ ), whereas if (all) the  $J=4$  praeodynium moments also order, one would expect  $\Delta c_{MF}$  to be larger by an amount between 4.5 R ( $g_J = 2$ ) and 7.3 R ( $g_J = 9$ ) (or an intermediate value if its orbital moment is quenched,  $L=0$ , and  $S=1$ ). Hence, our results, consistent with the doping studies<sup>7</sup>, suggest that it is the spins of the ruthenium ions that order at  $T_N$ , although we cannot rule out ordering of the chain praeodyniums.

One reaches a similar conclusion from considering the entropy. Harada and Hinatsu<sup>6</sup> found a rather large transition entropy by assuming that the background (phonon) specific heat of

$Pr_3RuO_7$  was the same as that of  $La_3NbO_7$ , which, as they discuss, is a questionable estimate for such a high  $T_N$ . Instead, we more simply fit the specific heat near the anomaly with a cubic

baseline, shown in Figure 3, to obtain a *very rough* estimate of the transition entropy,

$\Delta S = \int dT \Delta C/T \sim 0.5$  R. For mean-field theory,  $\Delta S_{MF} = v_N R \ln(g_J)$ , which would vary between 2.1 R and 6.6 R for (complete) praeodynium ordering and 0.7 R and 1.6 R for ruthenium ordering.

The low temperature specific heat is shown in Figure 4. In the inset, we plot  $c_P$  vs.  $T$ , while  $c_P/T$  vs.  $T^2$  is plotted in the main figure. For temperatures between 12 K and 20 K, the specific heat can be well represented by  $c_P = \gamma T + \beta T^3$ , with slope  $\beta \sim 120$  mJ mol<sup>-1</sup> K<sup>-4</sup>, as also observed by Zhou *et al*<sup>7</sup> for their powder sample. If entirely due to phonons, this would give a (per atom) Debye temperature of  $\Theta_D \sim 300$  K, but the  $\beta T^3$  term presumably also has a

contribution from antiferromagnetic magnons, which would increase  $\Theta_D$ . From the data above 12 K, one would also estimate  $\gamma \sim 160 \text{ mJ mol}^{-1} \text{ K}^{-2}$ , even larger than the electronic specific heat coefficient observed in highly correlated metallic ruthenates with the Ruddlesden-Popper structure<sup>15</sup>. Remarkably, an unusually large  $\gamma$  is also observed in insulating  $\text{Gd}_2\text{RuO}_5$ <sup>16</sup>. Indeed, if one assumes that the  $\chi_o$  term in the susceptibility is also due to conduction electrons, one finds a Wilson ratio of 0.94 for the ab-plane and only 0.71 for the c-axis. These small values in what would presumably be a strongly correlated conductor again suggest that both  $\chi_o$  and  $\gamma$  do not originate from a “hidden” Fermi surface in this nonconductor, e.g.  $\chi_o$  may be a van Vleck contribution.

In fact, we also observe a plateau in  $c_P$  at low temperature (see the inset), so that  $c_P/T$  starts increasing below 10 K; Zhou *et al*<sup>7</sup> observe a somewhat smaller increase (and no  $\gamma T$  term). This upturn in  $c_P/T$  can give rise to our apparent  $\gamma T$  term. For example, it may be due to ordering of spins not ordered at the Neel transition, i.e. all or some of the praesodynium ions. Consequently, we fit the low temperature specific heat to the Schottky expression

$c_P = \beta T^3 + v_S g (\delta/T)^2 \exp(\delta/T) / [1 + g \exp(\delta/T)]^2$ , where  $\delta$  is the excited state energy,  $g$  is the ratio of degeneracies of the ground state and excited state, and  $v_S$  is the number of ordering spins/unit cell.

The solid curve in the Figure 4 shows the fit with  $\gamma = 0$  and  $v = 3$  (appropriate to ordering of all the praesodynium ions), yielding  $\beta = 110 \text{ J mol}^{-1} \text{ K}^{-4}$  and  $\delta = 13.1 \text{ K}$ . If we assume a  $\text{Pr}^{3+}$  magnetic moment of  $3.6 \mu_B^6$ , this would imply an effective internal field of 2.7 T. However, this fit also has the unlikely value of  $g \sim 7$ , i.e. a ground state with high degeneracy (or with additional splittings much less than  $\delta$ ). Because the Schottky peak scales  $\sim v_S/g$ , reducing  $g$  will also reduce  $v_S$ . For example, the dashed curve shows a fit with  $v_S = 1$ , e.g. appropriate to

ordering of the chain praesodymium ions only. For this fit,  $\beta = 110 \text{ J mol}^{-1} \text{ K}^{-4}$ , and  $\delta = 13.9 \text{ K}$ , and  $g \sim 2$ . To reduce  $g$  to a value  $\leq 1$  would also reduce  $v_s \leq 0.5$ , which would imply the presence of a magnetic supercell, which has not yet been observed. This situation is not improved by allowing  $\gamma \neq 0$ , as this would force  $v_s/g$  to decrease.

Despite these uncertainties associated with the degeneracy, it seems plausible that the plateau in the low temperature specific heat can be accounted for with one or more Schottky terms, associated with  $\sim 10 \text{ K}$  crystal field splittings for the some or all of the  $\text{Pr}^{3+}$  ions.

#### 4. Conclusions

In summary, we present measurements of the magnetic and thermal properties of crystals of the spin-chain compound,  $\text{Pr}_3\text{RuO}_7$ . The material undergoes a Neel transition at  $T_N = 54 \text{ K}$  which is unusual in its degree of anisotropy and apparent mean-field behavior. The anisotropy and competing interactions result in a metamagnetic transition for fields along the chain direction. Both the specific heat and magnetization suggest that it is the ruthenium spins, perhaps augmented by some of the praesodymium moments, which order at  $T_N$ . The resulting internal field may cause ordering of remaining praesodymium spins at lower temperature, resulting in a Schottky anomaly in the specific heat.

This research was supported by the National Science Foundation. Grants # DMR-0100572, DMR-0240813, and DMR-0400938.

## References

<sup>1</sup> J. G. Allpress and H. J. Rossell, J. Solid State Chem. **27**, 105 (1979).

<sup>2</sup> D. Harada and Y. Hinatsu, J. Solid State Chem. **158**, 245 (2001)

<sup>3</sup> D. Harada, Y. Hinatsu, and Y. Ishii, J. Phys.: Condens. Matter **13**, 10825 (2001).

<sup>4</sup> P. Khalifah, R. W. Erwin, J. W. Lynn, Q. Huang, B. Batlogg, and R.J. Cava, Phys. Rev. B **60**, 9573 (1999).

<sup>5</sup> F. Wiss, N. P.Raju, A. S. Wills, and J.E. Greedan, Int. J. Inorg. Mater. **2**, 53 (2000).

<sup>6</sup> D. Harada and Y. Hinatsu, J. Solid State Chem. **164**, 163 (2002).

<sup>7</sup> Z. X. Zhou, G. Cao, S. McCall, J.E. Crow, R.P. Guertin, C.H. Mielke, and D.G. Rickel, Phil. Mag. **82**, 1401 (2002).

<sup>8</sup> G. Grüner, Rev. Mod. Phys. **66**, 1 (1994).

<sup>9</sup> J. P. Boucher and L. P. Regnault, J. Phys. I **6**, 1939 (1996).

<sup>10</sup> F. D. M. Haldane, Phys. Rev. Lett. **50**, 1153 (1983).

<sup>11</sup> E. Stryjewski and N. Giordano, Advances in Physics, **26**, 487 (1977).

<sup>12</sup> M. Chung, E. Figueroa, Y.-K. Kuo, Y. Wang, J.W. Brill, T. Burgin, and L.K. Montgomery, Phys. Rev. B **48**, 9256 (1993).

<sup>13</sup> Y. Wang, M. Chung, T.N. O'Neal, and J.W. Brill, Synth. Met. **46**, 307 (1992).

<sup>14</sup> H. Eugene Stanley, *Introduction to Phase Transitions and Critical Phenomena*, p. 89 (Oxford University Press, New York, 1971).

<sup>15</sup> X.N. Lin, V.A. Bondarenko, G. Cao, and J.W. Brill, Solid State, Commun. **130**, 151 (2004); T. Kiyama, K Yoshimura, K. Kosuge, H. Michor, and G. Hilscher, J. Phys. Soc. Jpn. **67**, 307 (1998); P.B. Allen, H. Berger, O. Chauvet, L. Forro, T. Jarlborg, A. Junod, B. Revaz, and G.

Santi, Phys. Rev. B **53**, 4393 (1996).

<sup>16</sup> G. Cao, S. McCall, S. Alexander, Z.X. Zhou, J.E. Crow and R.P. Guertin, Phys. Rev. B **63**, 144427 (2001)

## Figure Captions

**Fig.1.** The magnetic susceptibility  $\chi$  (defined as  $M/B$ ) as a function of temperature for  $\chi_{\parallel}$  and  $\chi_{\perp}$  at  $B=0.01$  T. Inset:  $\Delta\chi^{-1}$  vs.  $T$  where  $\Delta\chi \equiv \chi - \chi_0$ ; note that dots are the data, and solid lines are guides to the eye.

**Fig.2.** The isothermal magnetization  $M(B)$  at  $T=2$  K for  $M_{\parallel}$  and  $M_{\perp}$ .

**Fig.3.** The specific heat vs. temperature near  $T_N$ . The smooth curve shows the background discussed in the text; Inset: The specific heat over the entire temperature range (solid curve) and the differential scanning calorimetry results (dashed curve).

**Fig.4.** The low-temperature specific heat, plotted as  $c_p/T$  vs  $T^2$ , with the Schottky anomaly fits discussed in the text. The inset shows  $c_p$  vs.  $T$ .

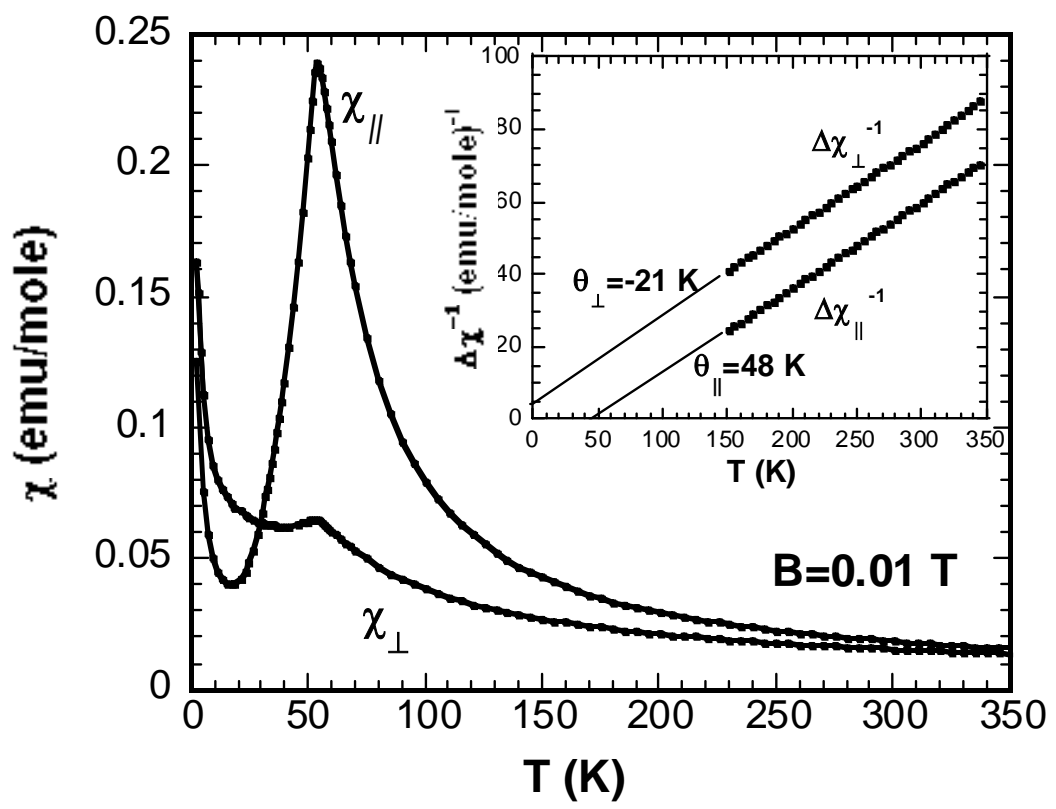


Figure 1

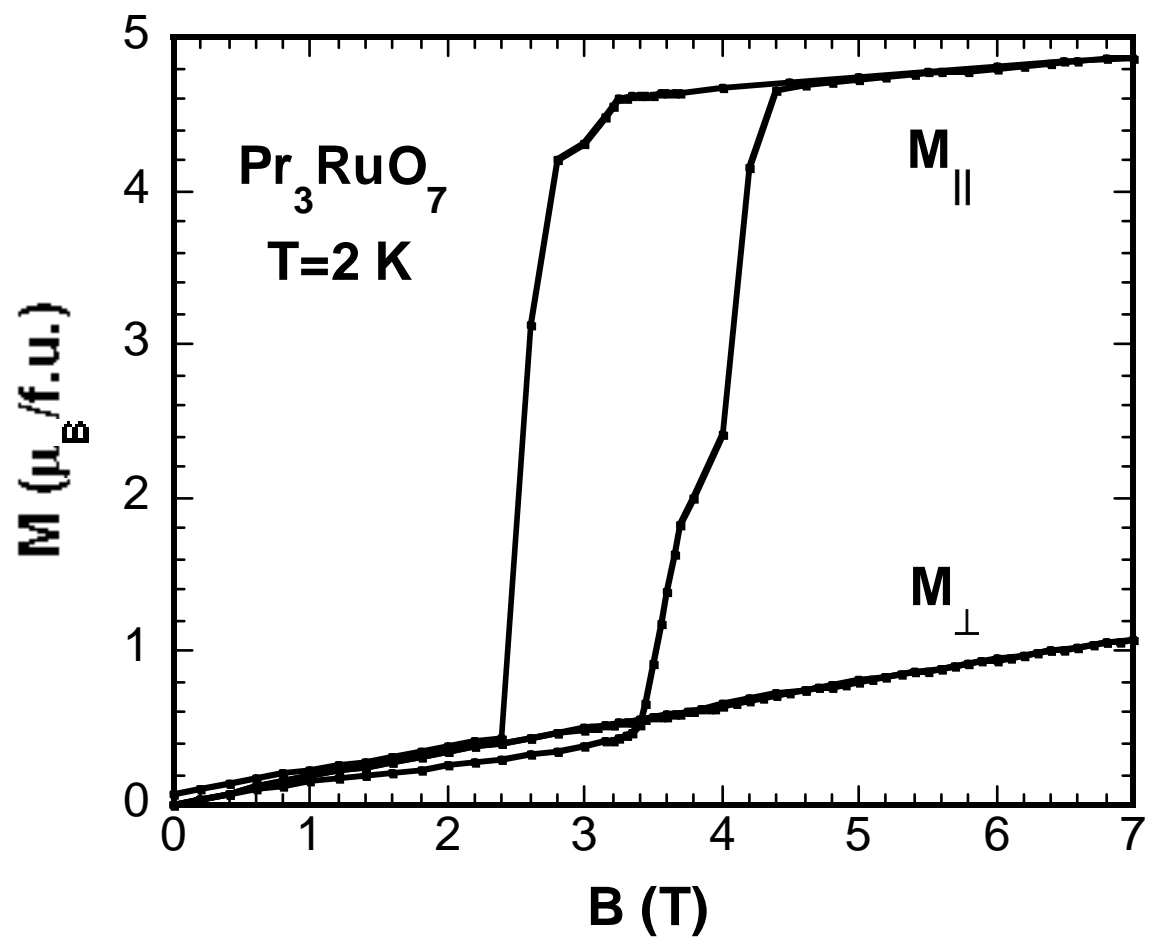


Figure 2

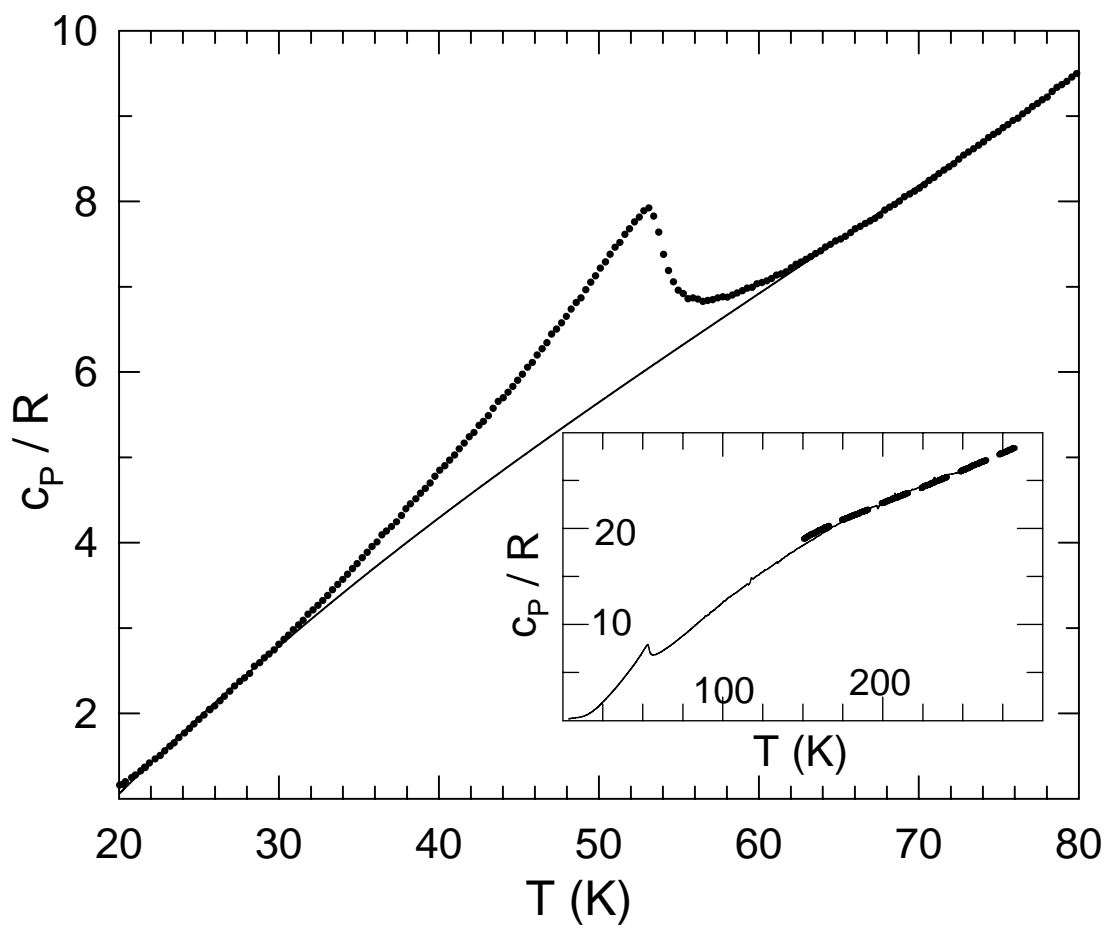


Figure 3

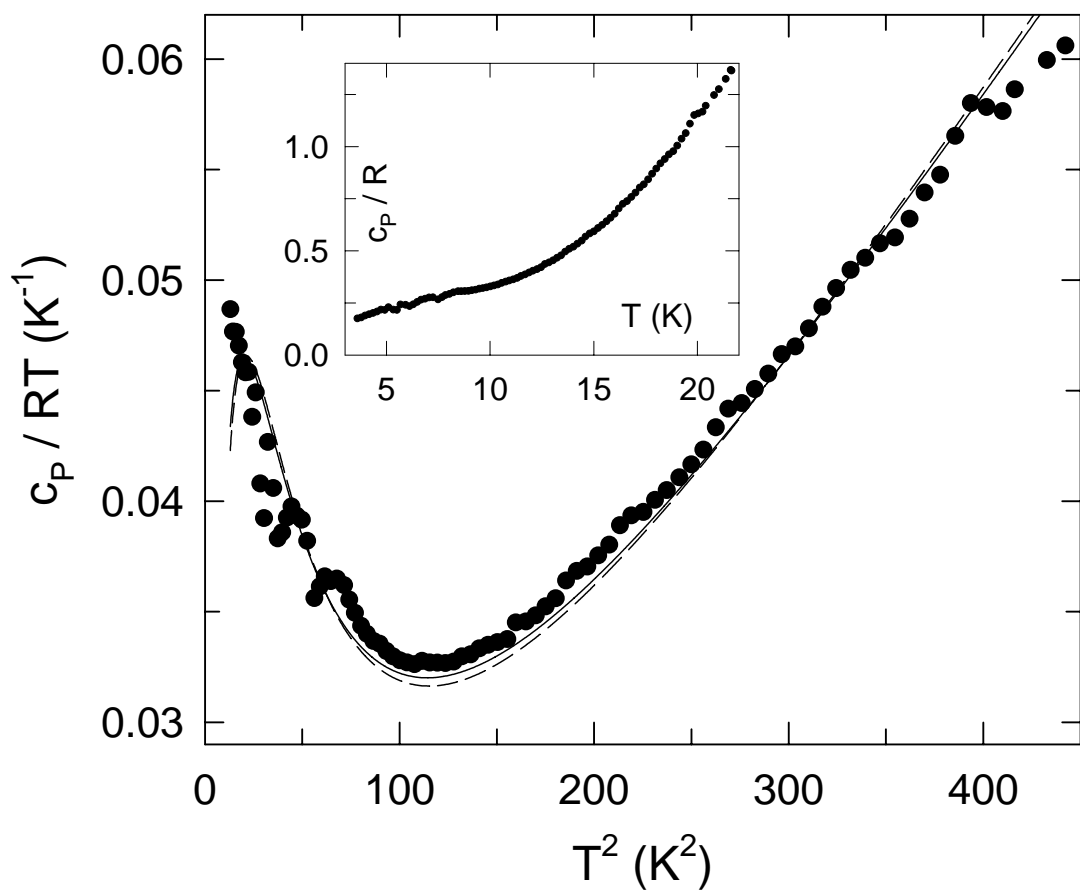


Figure 4